New Journal of Physics
The open-access journal for physics

Variational ground states of the two-dimensional Hubbard model

D Baeriswyl[1], D Eichenberger and M Menteshashvili
Department of Physics, University of Fribourg, CH-1700 Fribourg, Switzerland
E-mail: dionys.baeriswyl@unifr.ch

New Journal of Physics **11** (2009) 075010 (17pp)
Received 23 March 2009
Published 23 July 2009
Online at http://www.njp.org/
doi:10.1088/1367-2630/11/7/075010

Abstract. Recent refinements of analytical and numerical methods have improved our understanding of the ground-state phase diagram of the two-dimensional (2D) Hubbard model. Here, we focus on variational approaches, but comparisons with both quantum cluster and Gaussian Monte Carlo methods are also made. Our own ansatz leads to an antiferromagnetic ground state at half filling with a slightly reduced staggered order parameter (as compared to simple mean-field theory). Away from half filling, we find d-wave superconductivity, but confined to densities where the Fermi surface passes through the antiferromagnetic zone boundary (if hopping between both nearest-neighbour and next-nearest-neighbour sites is considered). Our results agree surprisingly well with recent numerical studies using the quantum cluster method. An interesting trend is found by comparing gap parameters Δ (antiferromagnetic or superconducting) obtained with different variational wave functions. Δ varies by an order of magnitude and thus cannot be taken as a characteristic energy scale. In contrast, the order parameter is much less sensitive to the degree of sophistication of the variational schemes, at least at and near half filling.

[1] Author to whom any correspondence should be addressed.

Contents

1. Introduction

The conventional mechanism of Cooper pairing rests on phonon exchange, but the case of superfluid ^{3}He shows that no additional degrees of freedom are necessary for establishing pairing, even in a system of fermions with predominantly repulsive interactions. Several years before the discovery of superfluidity in ^{3}He Kohn and Luttinger used perturbation theory to show that even a purely repulsive bare interaction can lead to an effective attraction in a channel with large enough angular momentum [1]. An analogous situation may prevail in superconducting cuprates, as suggested by Anderson as early as 1987 [2]. The Hubbard Hamiltonian with a large on-site repulsion U is indeed the natural model for describing the antiferromagnetic Mott insulator of undoped cuprates. Clearly there are phonons in these materials and the electron–phonon coupling can be rather strong, as suggested by optical spectroscopy [3], but a thorough treatment of both strong correlations and electron–phonon coupling is required to understand to what extent phonons affect the electronic properties in the cuprates. A recent debate [4, 5] on the origin of a kink observed in photoemission experiments demonstrates that such an analysis is still lacking. Correspondingly, the role of phonons in the superconductivity of cuprates also remains unclear.

In this paper, we restrict ourselves to the two-dimensional (2D) Hubbard model, described by the Hamiltonian

$$\hat{H} = \hat{H}_0 + U\hat{D}, \tag{1}$$

where

$$\hat{H}_0 = -\sum_{ij\sigma} t_{ij} c^\dagger_{i\sigma} c_{j\sigma} \tag{2}$$

describes hopping over the sites of a square lattice and

$$\hat{D} = \sum_i n_{i\uparrow} n_{i\downarrow} \tag{3}$$

measures the number of doubly occupied sites. The operator $c_{i\sigma}$ ($c^\dagger_{i\sigma}$) annihilates (creates) an electron at site i with spin σ and $n_{i\sigma} = c^\dagger_{i\sigma} c_{i\sigma}$. Only hopping between nearest ($t_{ij} = t$) and next-nearest neighbours ($t_{ij} = t'$) will be considered.

For small U the approach of Kohn and Luttinger looks promising, but naive perturbation theory diverges and one has to sum entire diagram classes (see [6] for a pedagogical treatment

of this problem). Moreover, there are several competing instabilities close to half filling, in particular, d-wave superconductivity and antiferromagnetism, or rather spin-density waves (SDWs). The problem can be solved in an elegant way using the functional renormalization group [7]–[10], which treats the competing density-wave and superconducting instabilities on the same footing. The specific techniques used by the different groups to calculate effective vertices and susceptibilities differ in details, but the overall results are more or less consistent, with an antiferromagnetic instability at half filling and d-wave superconductivity away—but not too far away—from half filling.

In the large-U limit, where double occupancy is suppressed, the Hubbard model can be replaced by the Heisenberg model at half filling [11] and by the t–J model close to half filling [12], defined by the Hamiltonian

$$\hat{H}_{t-J} = -\sum_{ij\sigma} t_{ij}\hat{P}_0 c^{\dagger}_{i\sigma} c_{j\sigma}\hat{P}_0 + \sum_{ij} J_{ij}\left(\boldsymbol{S}_i\cdot\boldsymbol{S}_j - \frac{1}{4}n_i n_j\right), \tag{4}$$

where $n_i = n_{i\uparrow} + n_{i\downarrow}$ counts the number of electrons at site i, the projector

$$\hat{P}_0 = \prod_i (1 - n_{i\uparrow}n_{i\downarrow}) \tag{5}$$

eliminates configurations with doubly occupied sites, $\boldsymbol{S}_i$ are spin $\frac{1}{2}$ operators and $J_{ij} = 2t_{ij}^2/U$.

While the ground state of the 2D Heisenberg model is fairly well understood [13]—it is widely accepted that it exhibits long-range antiferromagnetic order with a reduced moment due to quantum fluctuations—the ground state of the t–J model remains an unsolved problem, despite an extensive use of sophisticated methods during the last two decades [14, 15]. A simple ansatz

$$|\Psi\rangle = \hat{P}_0|\Psi_0\rangle, \tag{6}$$

is frequently used, where $|\Psi_0\rangle$ is the ground state of a suitable single-particle Hamiltonian, representing for instance the filled Fermi sea, a SDW or a superconductor. In a large region of doping the most favourable mean-field state $|\Psi_0\rangle$ has been found to be a superconducting ground state with d-wave symmetry [16]–[19]. In this case the ansatz (6) describes a resonating valence bond (RVB) [20] state, jokingly referred to as the 'plain vanilla version of RVB' [21].

Sometimes the t–J model is used to provide a simple argument for pairing. If the exchange coupling J is larger than the hopping amplitude t then it is favourable for two holes to remain nearest neighbours. Unfortunately, this is an unphysical limit for the Hubbard model for which the t–J model is only a valid approximation for $J \ll t$.

Experiments on layered cuprates indicate that U is neither small enough for a perturbative treatment nor large enough for the mapping to the t–J model. Thus, neutron scattering experiments on undoped cuprates [22] can be very well interpreted in terms of the 2D Hubbard model with U between $8t$ and $10t$ (depending on the approximation used for the magnon spectrum [23, 24]), in agreement both with an analysis of Raman data [25] and with a comparison between theoretical and experimental optical absorption spectra [26]. As to the 'kinetic' term $\hat{H}_0$, angular-resolved photoemission experiments [27, 28] give evidence for a hole-like Fermi surface, which can be described by taking both nearest-neighbour and next-nearest-neighbour hopping terms into account [29, 30]; the experiments are consistent with $t' \approx -0.3t$.

A lot of effort has been spent to treat the Hubbard model in the crossover regime of moderately large U. Quantum Monte Carlo methods have been developed in the 1980s, but

they suffer from severe statistical uncertainties at low temperatures and for large system sizes, both for many-fermion and quantum spin Hamiltonians [31]. This 'minus sign problem' turns out to be intrinsically hard [32]. The recently introduced Gaussian quantum Monte Carlo method [33] leads to positive weights, but the method is not immune to systematic errors [34]. Quantum cluster methods, which replace the single site of the dynamical mean-field theory [35] by a cluster of several sites, offer a promising alternative route for the intermediate-U regime [36, 37]. However, the spatial extent of the cluster that is treated essentially exactly has so far been very small (2×2). The large changes found in the case of the Mott transition when proceeding from a single site to a (2×2) cluster [38] indicate that larger cluster sizes are needed to obtain accurate results.

Alongside quantum Monte Carlo and quantum cluster methods, variational schemes have played a major role in the search of possible ground states of many-body systems. In the context of the Hubbard model, many variational wave functions go back to the ansatz of Gutzwiller [39]

$$|\Psi_{\mathrm{G}}\rangle = \mathrm{e}^{-g\hat{D}}|\Psi_0\rangle, \tag{7}$$

where the variational parameter g reduces double occupancy, weakly for small U and completely for $U \to \infty$. In spite of the simplicity of the ansatz, a substantial part of the correlation energy is obtained for small values of U. At half filling, the variational ground-state energy tends to the exact limiting value 0 for $U \to \infty$, where double occupancy is suppressed ($g \to \infty$) and the ansatz (7) coincides with the RVB state (6). Nonetheless many properties such as spin–spin correlation functions are described rather poorly, especially in the large-U regime. Several improvements have been proposed in terms of additional operators in front of the Gutzwiller ansatz, either to enhance magnetic or charge correlations [40, 41] or to increase the tendency of empty and doubly occupied sites to be next to each other [42, 43]. Very recently more elaborate states have been proposed, one including backflow [44], the other introducing a large number of variational parameters, both into $|\Psi_0\rangle$ and into the (Gutzwiller–Jastrow) correlation factor [45].

The main purpose of this paper is to describe our own variational ansatz in some more detail than previously [46, 47] and to compare our results with those of other approaches. In section 2, our ansatz is defined and shown to recover Anderson's RVB state in the large-U limit and for small hole doping. Section 3 analyses various wave functions for the Hubbard model on a four-site plaquette. For the square lattice, a variational Monte Carlo method is used to study our ansatz. The procedure is explained in section 4 and applied to an antiferromagnetic state at half filling. Our results for superconductivity away from half filling are presented in section 5 and compared to those of other variational wave functions and also to a very recent computation using a quantum cluster method. We do find evidence for a superconducting ground state, with an interesting hint at a magnetic mechanism. The concluding section 6 gives a brief summary of our main results.

2. Variational ground states

The primary effect of the Gutzwiller variational state (7) is the increased suppression of double occupancy as a function of U. Alternatively, we may motivate the ansatz as follows. Consider a general Hamiltonian $\hat{H} = \hat{H}_0 + \hat{H}_{\mathrm{int}}$, where $\hat{H}_0$ is a single-particle operator and $\hat{H}_{\mathrm{int}}$ the

interaction term. The state

$$|\Psi_\lambda\rangle = \mathrm{e}^{-\lambda \hat{H}}|\Psi_\mathrm{t}\rangle \tag{8}$$

tends to the exact ground state $|\Psi\rangle$ of $\hat{H}$ for $\lambda \to \infty$ (or to one of the ground states in the case of degeneracy) unless the trial state $|\Psi_\mathrm{t}\rangle$ is orthogonal to $|\Psi\rangle$. If $|\Psi_\mathrm{t}\rangle$ does not differ too much from $|\Psi\rangle$, a small parameter λ may be sufficient to obtain a good approximation. In this case we can make the replacement

$$\mathrm{e}^{-\lambda \hat{H}} \approx \mathrm{e}^{-\lambda \hat{H}_\mathrm{int}}\, \mathrm{e}^{-\lambda \hat{H}_0}. \tag{9}$$

Choosing $|\Psi_\mathrm{t}\rangle = |\Psi_0\rangle$, the ground state of $\hat{H}_0$, and treating λ as a variational parameter, we recover the Gutzwiller ansatz (7) in the case of the Hubbard model. At the same time this derivation indicates that the Gutzwiller ansatz is best suited for small values of U.

The factorization (9) is not unique, we may also choose

$$\mathrm{e}^{-\lambda \hat{H}} \approx \mathrm{e}^{-\lambda \hat{H}_0}\, \mathrm{e}^{-\lambda \hat{H}_\mathrm{int}}. \tag{10}$$

With $|\Psi_\mathrm{t}\rangle = |\Psi_0\rangle$ we arrive at an ansatz where both exponentials have to be kept. Allowing them to vary independently, we obtain

$$|\Psi_\mathrm{GB}\rangle = \mathrm{e}^{-h\hat{H}_0/t}\, \mathrm{e}^{-g\hat{D}}|\Psi_0\rangle. \tag{11}$$

The operator $\mathrm{e}^{-g\hat{D}}$ partially suppresses double occupancy for $g > 0$, while $\mathrm{e}^{-h\hat{H}_0/t}$ promotes both hole motion and kinetic exchange. The limit $h \to 0$ leads back to the Gutzwiller ansatz. The variational state (11) has been introduced by Otsuka [48] and studied both in 1D and in 2D. He found a substantial improvement with respect to the Gutzwiller ansatz. Moreover, $|\Psi_\mathrm{GB}\rangle$ has a large overlap with the exact ground state for all values of U in 1D, whereas on a square lattice this is only true for relatively small values of U (smaller than the bandwidth).

For $g \to \infty$ and $h \ll 1$, the ansatz (11) leads to the t–J model. To see this, we consider the limit $U \to \infty$, where $\mathrm{e}^{-g\hat{D}}|\Psi_0\rangle$ is replaced by the rhs of (6). The expectation value of the energy is then given by

$$E = \frac{\left\langle \Psi_0 \left| \hat{P}_0 \mathrm{e}^{-h\hat{H}_0/t} \left(\hat{H}_0 + U\hat{D}\right) \mathrm{e}^{-h\hat{H}_0/t} \hat{P}_0 \right| \Psi_0 \right\rangle}{\left\langle \Psi_0 \left| \hat{P}_0 \mathrm{e}^{-2h\hat{H}_0/t} \hat{P}_0 \right| \Psi_0 \right\rangle}. \tag{12}$$

At half filling the parameter h is equal to $-t/U$ in the large-U limit [49] and vanishes for $U \to \infty$. This remains valid very close to half filling, as we readily demonstrate. Expanding the expression (12) in powers of h, we obtain for the numerator

$$\left\langle \Psi_0 \left| \hat{P}_0 \mathrm{e}^{-h\hat{H}_0/t} \left(\hat{H}_0 + U\hat{D}\right) \mathrm{e}^{-h\hat{H}_0/t} \hat{P}_0 \right| \Psi_0 \right\rangle = \left\langle \Psi_0 \left| \hat{P}_0 \hat{H}_0 \hat{P}_0 \right| \Psi_0 \right\rangle - 2\frac{h}{t} \left\langle \Psi_0 \left| \hat{P}_0 \hat{H}_0^2 \hat{P}_0 \right| \Psi_0 \right\rangle + U\frac{h^2}{t^2} \left\langle \Psi_0 \left| \hat{P}_0 \hat{H}_0 \hat{P}_1 \hat{H}_0 \hat{P}_0 \right| \Psi_0 \right\rangle + \cdots, \tag{13}$$

where $\hat{P}_1$ is a projector onto the subspace with one doubly occupied site. For small doping, the operator $\hat{H}_0^2$ in the second term can be replaced by $\hat{H}_0 \hat{P}_1 \hat{H}_0$, and the denominator in (12) by 1. The minimization of the energy with respect to h then gives $h = -t/U$ and

$$E_\mathrm{min} \approx \langle \Psi_0 | \hat{P}_0 \left[\hat{H}_0 - \frac{1}{U} \hat{H}_0 \hat{P}_1 \hat{H}_0 \right] \hat{P}_0 | \Psi_0 \rangle. \tag{14}$$

Close to half filling, the second term in this expression can be rewritten as

$$\hat{P}_0\hat{H}_0\hat{P}_1\hat{H}_0\hat{P}_0 \approx 2\sum_{i,j} t_{ij}^2 \left(\frac{1}{4}n_i n_j - \boldsymbol{S}_i \cdot \boldsymbol{S}_j\right). \tag{15}$$

Thus we find indeed that in the limit $U \to \infty$ the variational treatment of the Hubbard model using the ansatz (11) is equivalent to the variational treatment of the t–J model using the ansatz (6). However, we have to keep in mind that the use of (11) for $g \to \infty$ is of doubtful validity. Therefore variational results obtained with the fully projected Gutzwiller wave function, as in the 'plain vanilla' RVB theory, have to be handled with care.

A complementary approach [49] starts from the ground state $|\Psi_\infty\rangle$ for $U \to \infty$, ideally the ground state of the t–J model close to half filling. Applying the same arguments as above, we obtain two new variational states,

$$\begin{aligned} |\Psi_{\mathrm{B}}\rangle &= \mathrm{e}^{-h\hat{H}_0/t}\,|\Psi_\infty\rangle, \\ |\Psi_{\mathrm{BG}}\rangle &= \mathrm{e}^{-g\hat{D}}\,\mathrm{e}^{-h\hat{H}_0/t}|\Psi_\infty\rangle, \end{aligned} \tag{16}$$

which should be well suited for describing the large-U regime. Unfortunately, it is in general very difficult to deal with the variational states $|\Psi_{\mathrm{B}}\rangle$ and $|\Psi_{\mathrm{BG}}\rangle$, because even an approximate calculation of $|\Psi_\infty\rangle$ represents already a highly nontrivial problem [50].

The trial states (7), (11) and (16) yield an appealing picture for the Mott metal–insulator transition as a function of U at half filling [51]–[54], where both $|\Psi_{\mathrm{G}}\rangle$ and $|\Psi_{\mathrm{GB}}\rangle$ represent metallic states, while $|\Psi_{\mathrm{B}}\rangle$ and $|\Psi_{\mathrm{BG}}\rangle$ are insulating. For the soluble 1D Hubbard model with long-range hopping, where $t_{ij} \sim |i-j|^{-1}$, the variational energies for $|\Psi_{\mathrm{G}}\rangle$ and $|\Psi_{\mathrm{B}}\rangle$ are dual to each other at half filling; similarly $|\Psi_{\mathrm{GB}}\rangle$ and $|\Psi_{\mathrm{BG}}\rangle$ form a dual pair [51]. On the metallic side (U smaller than the bandwidth) $|\Psi_{\mathrm{GB}}\rangle$ yields an order of magnitude improvement for the ground state energy as compared to $|\Psi_{\mathrm{G}}\rangle$, and the same effect is observed on the insulating side when $|\Psi_{\mathrm{B}}\rangle$ is replaced by $|\Psi_{\mathrm{BG}}\rangle$.

3. Lessons from the Hubbard square

The study of small clusters can provide useful benchmarks for variational wave functions. Clearly the cluster size should not be too small. In fact, for two particles on two sites both $|\Psi_{\mathrm{G}}\rangle$ and $|\Psi_{\mathrm{B}}\rangle$ yield the exact ground state, and there is no need to use more elaborate wave functions. Therefore, we proceed to the Hubbard square, an essentially 1D system when hopping is restricted to pairs of adjacent sites (figure 1(a)). We consider first the case of four particles and denote the corresponding ground state by $|\Psi^{(4)}\rangle$. A theorem by Lieb [55] directly implies that the ground state of the 1D Hubbard model for N particles on N sites is non-degenerate for any positive value of U and has total spin $S = 0$. For $U = 0$, the ground state of our Hubbard square is fourfold degenerate (for $S_z = 0$) with energy $E = -4t$, and one can use perturbation theory to determine the $U \to 0$ limit of $|\Psi^{(4)}\rangle$. Apart from $S = 0$, $|\Psi^{(4)}\rangle$ can be characterized by its transformation properties with respect to the symmetry group $\mathcal{D}_4$; it has total quasimomentum π (i.e. it is odd under the rotation of the square by the angle $\pi/2$ about the axis perpendicular to the plane of the square and passing through its centre), it is even with respect to reflections in a plane parallel to one of the sides and odd with respect to reflections in a plane passing through a diagonal. Denoting $d_i^\dagger := c_{i\uparrow}^\dagger c_{i\downarrow}^\dagger$ and $b_{ij}^\dagger := \frac{1}{\sqrt{2}}(c_{i\uparrow}^\dagger c_{j\downarrow}^\dagger - c_{i\downarrow}^\dagger c_{j\uparrow}^\dagger) = b_{ji}^\dagger$, the ground state can be

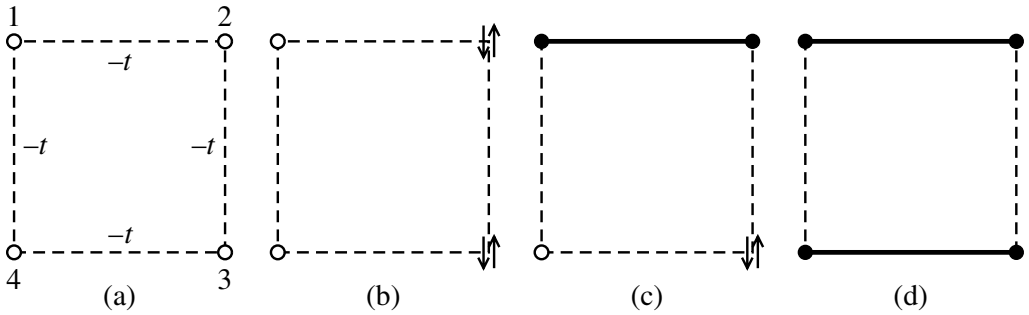

Figure 1. (a) Illustration of the Hubbard square; (b)–(d) representations of the three different types of configurations present in the ground state of the half-filled Hubbard square. The symbols stand for: ○ empty site, ●—● singlet bond, ↑↓ doubly occupied site.

written as

$$|\Psi^{(4)}\rangle = \frac{a|\Phi_2\rangle + b|\Phi_1\rangle + c|\Phi_0\rangle}{\sqrt{a^2+b^2+c^2}}, \tag{17}$$

with

$$|\Phi_2\rangle = \tfrac{1}{2}\left(d_1^\dagger d_2^\dagger - d_2^\dagger d_3^\dagger + d_3^\dagger d_4^\dagger - d_1^\dagger d_4^\dagger\right)|0\rangle,$$

$$|\Phi_1\rangle = \frac{1}{2\sqrt{2}}\left(d_1^\dagger b_{23}^\dagger - d_2^\dagger b_{34}^\dagger + d_3^\dagger b_{41}^\dagger - d_4^\dagger b_{12}^\dagger - d_1^\dagger b_{43}^\dagger + d_2^\dagger b_{14}^\dagger - d_3^\dagger b_{21}^\dagger + d_4^\dagger b_{32}^\dagger\right)|0\rangle,$$

$$|\Phi_0\rangle = \frac{1}{\sqrt{3}}\left(b_{14}^\dagger b_{23}^\dagger - b_{12}^\dagger b_{34}^\dagger\right)|0\rangle,$$

where $|0\rangle$ is the vacuum (zero-electron) state and a, b, c are real, U-dependent coefficients, whose analytical expressions are too cumbersome to be presented here. The states $|\Phi_D\rangle$, illustrated in figures 1(b)–(d), are eigenstates of $\hat{D}$ with $D = 0, 1, 2$ doubly occupied sites (doublons). With increasing U the weights of $|\Phi_1\rangle$ and $|\Phi_2\rangle$ decrease and vanish for $U \to \infty$. Therefore $|\Phi_0\rangle$ is equal to $|\Psi_\infty\rangle$, the normalized ground state of the Heisenberg model on the square with nearest-neighbour antiferromagnetic exchange. We also note that in the state $|\Phi_2\rangle$ the two doublons sit on adjacent sites of the square. Similarly, in the state $|\Phi_1\rangle$ the doublon and the holon (empty site) sit on adjacent sites of the square. The hopping operator $\hat{H}_0$ mixes the states $|\Phi_D\rangle$, but does not bring in other states.

As already noted by other authors [56], the ground state $|\Psi^{(4)}\rangle$ has an affinity for d-wave pairing. In fact, the quantity $\langle\Psi^{(4)}|C_\mathrm{d}C_\mathrm{d}^\dagger|\Psi^{(4)}\rangle$, where $C_\mathrm{d}^\dagger := \frac{1}{2}(b_{12}^\dagger - b_{23}^\dagger + b_{34}^\dagger - b_{41}^\dagger)$ creates a d-wave pair, is larger than the corresponding quantity for s-wave pairing, $\langle\Psi^{(4)}|C_\mathrm{s}C_\mathrm{s}^\dagger|\Psi^{(4)}\rangle$ with $C_\mathrm{s}^\dagger := \frac{1}{2}(b_{12}^\dagger + b_{23}^\dagger + b_{34}^\dagger + b_{41}^\dagger)$. The difference, especially prominent for small U, decreases with increasing U and tends to zero for $U \to \infty$. The ground state $|\Psi^{(4)}\rangle$ also exhibits local antiferromagnetic order, which is noticeably enhanced with increasing U.

Knowing the exact ground state, one can examine the quality of various variational wave functions. Figure 2(a) shows that the Gutzwiller ansatz $|\Psi_\mathrm{G}\rangle$ already yields a fairly good approximation for all values of U, with the biggest deviation for intermediate U ($\sim 4t$), where the variational energy deviates from the exact value by about 0.5%, whereas the overlap

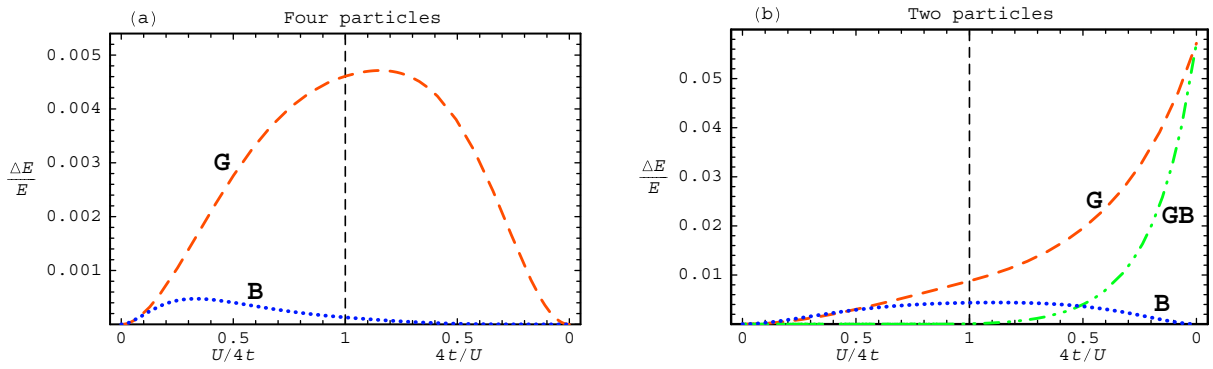

Figure 2. Relative deviation $\Delta E/E$ of different variational ground-state energies from the exact value E for the Hubbard square: (a) half filling and (b) quarter filling. The lines correspond to: – – – $|\Psi_{\mathrm{G}}\rangle$, · · · $|\Psi_{\mathrm{B}}\rangle$, — · · — $|\Psi_{\mathrm{GB}}\rangle$.

$\langle\Psi_{\mathrm{G}}|\Psi^{(4)}\rangle$ is still about 99.95%. The state $|\Psi_{\mathrm{B}}\rangle$, equation (16), is even better, with an improvement of one order of magnitude (or more) for $U > 2t$ as compared to $|\Psi_{\mathrm{G}}\rangle$. Generally speaking, since the wave function (17) has two independent coefficients, one needs, in principle, a variational wave function with at least two parameters to reproduce the exact ground state. Not all wave functions are equally successful, though. Both the refined Gutzwiller ansatz $|\Psi_{\mathrm{GB}}\rangle$ and its counterpart $|\Psi_{\mathrm{BG}}\rangle$ do give the exact ground state $|\Psi^{(4)}\rangle$ of the half-filled Hubbard square, but Kaplan's generalization [42] fails in doing so, because what should be suppressed by his additional operator (configurations with doublons having no holons on nearest-neighbour sites) is absent for the states $|\Phi_D\rangle$, $D = 0, 1, 2$. More involved variational states [45] can easily reproduce the exact ground state.

The ground state $|\Psi^{(2)}\rangle$ for two electrons on the four sites of a square is rather different. Its energy reaches the limiting value $E_\infty = -2\sqrt{2}\,t$ (and not 0) for $U \to \infty$. Its quasimomentum is 0 and the two particles form an s-wave pair. The quantity $\langle\Psi^{(2)}|C_{\mathrm{s}}C_{\mathrm{s}}^{\dagger}|\Psi^{(2)}\rangle$, expressing the affinity for s-wave pairing, dominates now over the corresponding d-wave expression, $\langle\Psi^{(2)}|C_{\mathrm{d}}C_{\mathrm{d}}^{\dagger}|\Psi^{(2)}\rangle$, for all values of U except for $U = 0$, where the two quantities are equal. The difference increases with U and reaches a maximum for $U \to \infty$.

$|\Psi^{(2)}\rangle$ can also be represented as a superposition of three components, but now only one of them contains real-space configurations with doubly occupied sites. As a result, the Gutzwiller ansatz $|\Psi_{\mathrm{G}}\rangle$ gives a fairly poor description of the state, it even predicts a wrong asymptotic value for the energy, $E_{\mathrm{G}} - E_\infty \approx 0.16t$ for $U \to \infty$ (figure 2(b)). The refined Gutzwiller ansatz $|\Psi_{\mathrm{GB}}\rangle$ is not perfect either, it reproduces the exact ground state only below a limiting value of $U \approx 3.46t$. Even if one adds a third operator $\mathrm{e}^{-g'\hat{D}}$ in front of $|\Psi_{\mathrm{GB}}\rangle$, the situation remains essentially the same. What needs to be done in order to achieve full coincidence with the exact ground state for all U is to use $\hat{P}_0\hat{H}_0\hat{P}_0$ instead of $\hat{H}_0$ in combination with the Gutzwiller factor, thereby ensuring that no more doublons are created by $\hat{H}_0$ after being suppressed by $\mathrm{e}^{-g\hat{D}}$.

On the other hand, $|\Psi_{\mathrm{B}}\rangle$ gives a more or less satisfactory approximation of the exact ground state, about as good as the Gutzwiller ansatz in the half-filled case. Adding to $|\Psi_{\mathrm{B}}\rangle$ any of the above-mentioned factors (Gutzwiller, doublon–holon correlations, Jastrow) gives full coincidence with the exact two-electron ground state.

The analysis of the Hubbard square confirms that proceeding from $|\Psi_G\rangle$ to $|\Psi_{GB}\rangle$ (or from $|\Psi_B\rangle$ to $|\Psi_{BG}\rangle$) improves substantially the variational ground state. Moreover, for $U \gtrsim t$ it is preferable to use $|\Psi_B\rangle$ ($|\Psi_{BG}\rangle$) as a variational ansatz, rather than $|\Psi_G\rangle$ ($|\Psi_{GB}\rangle$), i.e. it is advantageous to start from $|\Psi_\infty\rangle$, the ground state of the t–J model in the limit $J \to 0$ (or of the Heisenberg Hamiltonian at half filling).

4. Antiferromagnetism

We return now to the square lattice. The lessons from the Hubbard square suggest the use of $|\Psi_B\rangle$ or $|\Psi_{BG}\rangle$, but, unfortunately, the reference state $|\Psi_\infty\rangle$ is very difficult to handle, except for small clusters (using exact diagonalization). This is the main reason why $|\Psi_B\rangle$ and $|\Psi_{BG}\rangle$ have not been used so far for the square lattice. In the remainder of this paper we will therefore mostly be concerned with wave functions linked to $|\Psi_0\rangle$, the ground state of an appropriate mean-field Hamiltonian.

We first consider an antiferromagnetic ground state, restricting ourselves to the half-filled band case (number of particles N equal to the number of sites L). To enforce a commensurate SDW (with a preference for up spins on one sublattice and for down spins on the other), we introduce the mean-field Hamiltonian

$$\hat{H}_{\mathrm{mf}} = \hat{H}_0 - \Delta \sum_i (-1)^i (n_{i\uparrow} - n_{i\downarrow}), \tag{18}$$

where i is even on one sublattice and odd on the other. The staggered order parameter m is defined as

$$m := \frac{1}{2L} \sum_i (-1)^i \left\langle n_{i\uparrow} - n_{i\downarrow} \right\rangle, \tag{19}$$

where the expectation value is calculated with respect to the chosen trial state. The simplest case is the ground state of $\hat{H}_{\mathrm{mf}}$, a commensurate SDW with wave vector $\boldsymbol{Q} = (\pi, \pi)$.

The expectation value of the Hubbard Hamiltonian can be written as

$$\left\langle \hat{H} \right\rangle = \left\langle \hat{H}_{\mathrm{mf}} \right\rangle + 2L\Delta m + U \sum_i \left\langle n_{i\uparrow} n_{i\downarrow} \right\rangle. \tag{20}$$

For the trial state $|\mathrm{SDW}\rangle$, the ground state of $\hat{H}_{\mathrm{mf}}$, the average double occupancy is simply given by

$$\left\langle \mathrm{SDW} \left| n_{i\uparrow} n_{i\downarrow} \right| \mathrm{SDW} \right\rangle = \tfrac{1}{4} - m^2, \tag{21}$$

while the Hellman–Feynman theorem yields

$$\frac{\mathrm{d}}{\mathrm{d}\Delta} \left\langle \mathrm{SDW} \left| \hat{H}_{\mathrm{mf}} \right| \mathrm{SDW} \right\rangle = -2Lm. \tag{22}$$

Minimizing $\langle \hat{H} \rangle$ with respect to Δ and using (21) and (22), we obtain

$$(\Delta - Um) \frac{\mathrm{d}m}{\mathrm{d}\Delta} = 0, \tag{23}$$

and therefore

$$\Delta = Um. \tag{24}$$

The order parameter m is easily calculated for the mean-field state. The transformation

$$c_{k\sigma} = \frac{1}{\sqrt{L}} \sum_i \mathrm{e}^{-\mathrm{i}\boldsymbol{k}\cdot\boldsymbol{R}_i}\, c_{i\sigma}, \tag{25}$$

where the wave vectors $\boldsymbol{k}$ belong to the first Brillouin zone and $\boldsymbol{R}_i$, $i = 1, \ldots, L$, are lattice vectors (with lattice constant set to 1), diagonalizes the hopping term,

$$\hat{H}_0 = \sum_{k\sigma} \varepsilon_{\boldsymbol{k}}\, c^\dagger_{k\sigma} c_{k\sigma}\,, \tag{26}$$

with a spectrum

$$\varepsilon_{\boldsymbol{k}} = -2t\,(\cos k_x + \cos k_y) - 4t'\,\cos k_x\,\cos k_y. \tag{27}$$

In the rest of this section, we choose $t' = 0$ and thus obtain a spectrum with electron–hole symmetry,

$$\varepsilon_{\boldsymbol{k}} = -\varepsilon_{\boldsymbol{k}\pm\boldsymbol{Q}}. \tag{28}$$

In reciprocal space, the mean-field Hamiltonian reads

$$\hat{H}_{\mathrm{mf}} = \sum\nolimits'_{k\sigma} \left\{ \varepsilon_{\boldsymbol{k}} \left(c^\dagger_{k\sigma} c_{k\sigma} - c^\dagger_{k+Q,\sigma} c_{k+Q,\sigma} \right) - \sigma\Delta \left(c^\dagger_{k\sigma} c_{k+Q,\sigma} + c^\dagger_{k+Q,\sigma} c_{k\sigma} \right) \right\}, \tag{29}$$

where the notation $\sum'_{\boldsymbol{k}}$ means that the sum includes only half of the wave vectors of the Brillouin zone, those satisfying $\varepsilon_k \leqslant 0$. $\hat{H}_{\mathrm{mf}}$ is easily diagonalized by a Bogoliubov transformation. The spectrum (in the folded zone) is split into $\pm E_{\boldsymbol{k}}$, where

$$E_{\boldsymbol{k}} = \sqrt{\varepsilon^2_{\boldsymbol{k}} + \Delta^2}. \tag{30}$$

The order parameter is found to be

$$m = \frac{1}{L} \sum\nolimits'_k \frac{\Delta}{E_{\boldsymbol{k}}}. \tag{31}$$

The relations (24) and (31) determine both the gap parameter Δ and the order parameter m for the mean-field ground state $|\mathrm{SDW}\rangle$.

We now proceed to the correlated trial state

$$|\Psi_{\mathrm{GB}}\rangle = \mathrm{e}^{-h\hat{H}_0/t}\, \mathrm{e}^{-g\hat{D}}\, |\mathrm{SDW}\rangle. \tag{32}$$

To decouple the terms $n_{i\uparrow} n_{i\downarrow}$ in the operator $\mathrm{e}^{-g\hat{D}}$, a discrete Hubbard–Stratonovich transformation [57] is applied,

$$\begin{aligned} \mathrm{e}^{-g\hat{D}} &= \exp\left\{ -g \sum_i n_{i\uparrow} n_{i\downarrow} \right\} \\ &= \prod_i \cosh\left[2a \left(n_{i\uparrow} - n_{i\downarrow} \right) \right] \exp\left\{ -\frac{g}{2} \left(n_{i\uparrow} + n_{i\downarrow} \right) \right\} \\ &= 2^{-L} \sum_{\tau_1,\ldots,\tau_L} \exp\left\{ \sum_{i\sigma} \left(2a\sigma\tau_i - \frac{g}{2} \right) n_{i\sigma} \right\}, \end{aligned} \tag{33}$$

where τ_i are Ising variables assuming the values ± 1, and $a = \mathrm{arctg}\sqrt{\mathrm{th}(g/4)}$. As a result, both exponential operators in (32) are quadratic in fermionic creation and annihilation operators, and therefore the fermionic degrees of freedom can be integrated out [58]. We obtain the following expressions:

$$\langle \Psi_{\mathrm{GB}} | \hat{H} | \Psi_{\mathrm{GB}} \rangle = \sum_{\substack{\tau_1,\ldots,\tau_L \\ \tau'_1,\ldots,\tau'_L}} E\left(\tau_1, \ldots \tau_L; \tau'_1, \ldots, \tau'_L\right) ,$$

$$\langle \Psi_{\mathrm{GB}} | \Psi_{\mathrm{GB}} \rangle = \sum_{\substack{\tau_1,\ldots,\tau_L \\ \tau'_1,\ldots,\tau'_L}} N\left(\tau_1, \ldots \tau_L; \tau'_1, \ldots, \tau'_L\right) , \tag{34}$$

where the quantities $E(\tau_1, \ldots, \tau_L; \tau'_1, \ldots, \tau'_L)$ and $N(\tau_1, \ldots, \tau_L; \tau'_1, \ldots, \tau'_L)$ are products of determinants of $L/2 \times L/2$ matrices. (Initially, one has to deal with $L \times L$ matrices, but these can be block-diagonalized into two $L/2 \times L/2$ matrices because up and down spins are never mixed.)

The expectation value of the energy

$$E(g, h, \Delta) = \frac{\langle \Psi_{\mathrm{GB}} | \hat{H} | \Psi_{\mathrm{GB}} \rangle}{\langle \Psi_{\mathrm{GB}} | \Psi_{\mathrm{GB}} \rangle} \tag{35}$$

is then calculated by Monte Carlo sampling and minimized with respect to the three variational parameters g, h, Δ. The computations have been limited to an 8×8 lattice, with a fixed value of $U = 8t$.

It is instructive to follow the evolution of the results as the variational ground state is refined, from the simple SDW state $|\Psi_0\rangle = |\mathrm{SDW}\rangle$ via the Gutzwiller ansatz $|\Psi_{\mathrm{G}}\rangle = \mathrm{e}^{-g\hat{D}}|\mathrm{SDW}\rangle$ to $|\Psi_{\mathrm{GB}}\rangle = \mathrm{e}^{-h\hat{H}_0/t}\mathrm{e}^{-g\hat{D}}|\mathrm{SDW}\rangle$. The gap parameter Δ is found to decrease dramatically [46]. It amounts to about $3.6\,t$ for the plain SDW state, $1.3t$ for the Gutzwiller ansatz and $0.32t$ for $|\Psi_{\mathrm{GB}}\rangle$. This indicates that Δ has no clear physical meaning and cannot be simply related to an excitation gap for the correlated states $|\Psi_{\mathrm{G}}\rangle$ and $|\Psi_{\mathrm{GB}}\rangle$. We expect Δ to decrease steadily as the variational ansatz is further refined and to tend to zero as the trial state approaches the exact ground state. In fact, in this limit the gap parameter merely plays the role of an (infinitesimal) symmetry-breaking field.

In spite of the strong variation of Δ, the order parameter does not change much [46], from $m \approx 0.45$ for $|\mathrm{SDW}\rangle$ to $m \approx 0.43$ for $|\Psi_{\mathrm{G}}\rangle$ and $m \approx 0.39$ for $|\Psi_{\mathrm{GB}}\rangle$. Thus the result for our most sophisticated variational ansatz is higher than the extrapolation $m \approx 0.22$ from Monte Carlo simulations on relatively small lattices [59], and also higher than the value $m \approx 0.31$ extracted from large-scale Monte Carlo simulations [60] for the 2D spin-$\frac{1}{2}$ Heisenberg model (and expected to represent an upper limit for the antiferromagnetic order parameter of the Hubbard model).

Quite generally, the order parameter obtained within mean-field theory is reduced when quantum fluctuations are taken into account. Our results indicate that quantum fluctuations are progressively included when proceeding from the simple SDW state $|\mathrm{SDW}\rangle$ over $|\Psi_{\mathrm{G}}\rangle$ to $|\Psi_{\mathrm{GB}}\rangle$. Nonetheless, long-range (spin wave) fluctuations are suppressed by the gap Δ, which is small but still finite for $|\Psi_{\mathrm{GB}}\rangle$. It is interesting to note that a recent calculation using a quantum cluster method [61] gave $m \approx 0.4$, which agrees with our value. The small size of the cluster (2×2) used in these calculations suggests that long-range fluctuations are not properly taken into account either.

5. Superconductivity

We discuss now the region away from half filling, i.e. densities $n = N/L \neq 1$. We have tried to examine the fate of antiferromagnetism for $n \neq 1$, but so far our variational Monte Carlo approach did not converge fast enough to allow the extraction of reliable results. In the following we limit ourselves to superconducting ground states with d-wave symmetry. The mean-field state $|\Psi_0\rangle$ is constructed as a conventional Bardeen–Cooper–Schrieffer (BCS) state, with

$$\Delta(\boldsymbol{k}) = \Delta_0(\cos\, k_x - \cos\, k_y). \tag{36}$$

The variational calculations follow the same steps as in the SDW case, but now one has to deal with $2L \times 2L$ matrices because, in contrast to the SDW case, up and down spins are now mixed as are particles and holes.

Our trial state

$$|\Psi_{\mathrm{GB}}\rangle = \mathrm{e}^{-h\hat{H}_0/t}\mathrm{e}^{-g\hat{D}}|\mathrm{BCS}\rangle \tag{37}$$

has three variational parameters, h, g and Δ_0, as well as the parameter μ, which fixes the average number of electrons, but is not identical to the true chemical potential. Instead of this 'grand-canonical' set-up one could also work with a BCS state projected onto a fixed number of particles, where μ becomes a fourth variational parameter. Unfortunately, the minus sign problem turns out to be severe in the 'canonical' case [62], presumably because $|\mathrm{BCS}\rangle_N$ is a correlated state, whereas the conventional BCS wave function can be written as a single Slater determinant. The results discussed below have all been obtained using the grand-canonical version.

The calculations were mostly done for an 8×8 lattice, but in order to study the size dependence we have also made a few runs for 6×6 and 10×10 lattices. The results for an 8×8 and a 10×10 lattice do not differ considerably if the gap parameter Δ_0 is large enough [46], as is the case for $n = 0.90$ and 0.94. For $n = 0.84$, the finite size effects are still rather strong.

As in the case of antiferromagnetism, the gap parameter Δ_0 varies strongly as the trial wave function is refined. Thus, the fully Gutzwiller-projected BCS state, used as an ansatz for the t–J model [18], gives large values in an extended region of densities. Within this approximation, the largest gap parameter, $\Delta_0 \approx t$, is found at half filling, followed by a nearly linear decrease as a function of doping concentration $x = 1 - n$, until Δ_0 vanishes at $x_{\mathrm{c}} \approx 0.35$. Similar behaviour is found for $|\Psi_{\mathrm{G}}\rangle$ applied to the Hubbard model [46], but with a smaller critical density and a reduced value at $x = 0$, $\Delta_0 \approx 0.2t$. The gap is reduced still further when proceeding from $|\Psi_{\mathrm{G}}\rangle$ to $|\Psi_{\mathrm{GB}}\rangle$ [46], with a maximum of $0.13t$ for $x \approx 0.1$ and a critical hole density $x_{\mathrm{c}} \approx 0.18$. It is worthwhile to mention that a Gutzwiller ansatz with coexisting antiferromagnetism and superconductivity also produces a maximum in the gap parameter as a function of density [63], $\Delta_0 \approx 0.1t$ at $x \approx 0.1$.

For the repulsive Hubbard model, the superconducting order parameter Φ is commonly chosen as the expectation value of a pair of creation operators on neighbouring sites,

$$\Phi = \left\langle c^{\dagger}_{i\uparrow} c^{\dagger}_{i+\tau\downarrow} \right\rangle. \tag{38}$$

For d-wave symmetry, Φ has a different sign for a horizontal bond than for a vertical bond. Alternatively, one can extract the order parameter from the correlation function

$$S_{\tau\tau'}\left(\boldsymbol{R}_i - \boldsymbol{R}_j\right) = \left\langle c_{i+\tau\downarrow} c_{i\uparrow} c^{\dagger}_{j\uparrow} c^{\dagger}_{j+\tau'\downarrow} \right\rangle \tag{39}$$

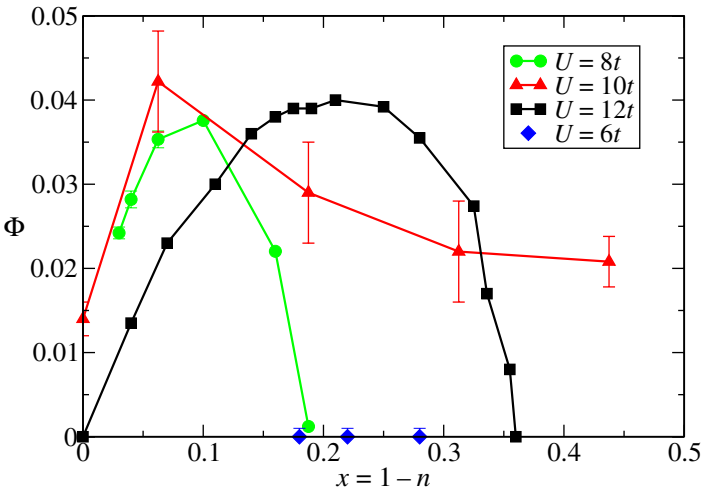

Figure 3. Comparison of superconducting order parameters for the simple Hubbard model and four different approaches: full Gutzwiller projection for the t–J model ($U = 12\,t$, ■—■), partial Gutzwiller projection ($U = 10\,t$, ▲—▲), our ansatz ($U = 8\,t$, ●—●) and Gaussian Monte Carlo ($U = 6\,t$, ◆).

for $|\boldsymbol{R}_i - \boldsymbol{R}_j| \to \infty$. For the exact ground state, the two procedures, the evaluation of (38) for an infinitesimal symmetry breaking on the one hand, and the determination of the asymptotic behaviour of the correlation function (39) on the other, are expected to yield the same order parameter Φ in the thermodynamic limit ($N, L \to \infty$ for constant density n).

We first discuss results for $t' = 0$. Figure 3 shows the d-wave order parameter as a function of doping, $x = 1 - n$, obtained following four different routes. Three of them are variational, full Gutzwiller projection for the t–J model (black squares) [18], the Gutzwiller ansatz, including a finite antiferromagnetic order parameter close to half filling (red triangles) [63] and our ansatz (37) (green circles) [46]. The null result (blue diamonds) is from recent (Gaussian) Monte Carlo simulations of Aimi and Imada [64], who extracted tiny upper bounds for the order parameter from the long-distance behaviour of the correlation function (39). Unfortunately, the four data sets were obtained for four different values of U. Nonetheless, the three variational results are remarkably similar for weak doping ($x \lesssim 0.1$). For $x \gtrsim 0.18$, there appears to be a discrepancy between the results of [63] and our results. Note that the Gutzwiller data [63] have been obtained on the basis of the correlation function (39), which is expected to yield a finite order parameter for a finite system, even if there is no long-range order in the thermodynamic limit. Therefore the apparent discrepancy may be an artefact of the procedure, as pointed out in [63]. This is confirmed by our own results for the Gutzwiller trial state $|\Psi_{\mathrm{G}}\rangle$, where we find [58] that the extrapolation of the order parameter for $L \to \infty$ gives $\Phi \to 0$ for $x \gtrsim 0.2$, in agreement with our results for $|\Psi_{\mathrm{GB}}\rangle$. Clearly our ansatz $|\Psi_{\mathrm{GB}}\rangle$ should be superior to the Gutzwiller wave function, either partially or fully projected. It is worthwhile to mention that refined variational states for the t–J model [50] did not give markedly different results from those presented in figure 3 for the fully Gutzwiller-projected wave function. Therefore there seems to be a clear difference between the Hubbard and t–J model predictions for superconductivity above, say, a doping concentration of 18%, where superconductivity appears

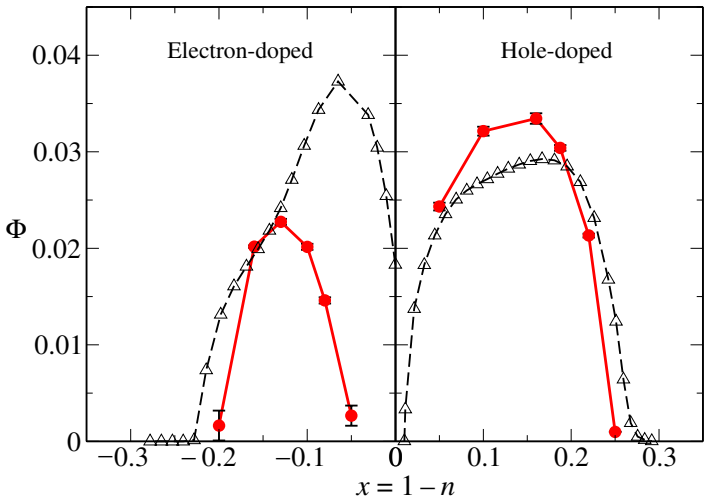

Figure 4. Superconducting order parameter as a function of doping for the Hubbard model including next-nearest-neighbour hopping: ●—● our variational data, △—△ results obtained with the quantum cluster method. All data points were obtained using the parameter values $U = 8t$, $t' = -0.3t$.

to be absent for the Hubbard model, but to persist up to about 40% for the t–J model. This is not a true discrepancy because the mapping from the large-U Hubbard model to the t–J model is only justified close to half filling. Figure 3 also shows that there is no disagreement between our variational result [46] and the Gaussian Monte Carlo data [64], which so far are only available for $x \gtrsim 0.18$.

We turn now to the more realistic case of hopping between both nearest and next-nearest neighbours. Figure 4 compares our variational results (red circles) [47] with recent data obtained with the quantum cluster method (open triangles) [61]. The same parameter sets ($U = 8t$, $t' = -0.3t$) were used in both approaches. The agreement is remarkably good, in view of the fact that the two methods are very different. Only the surprising peak found in the quantum cluster approach for an electron doping of about 5% is absent in our variational data. This peak is suppressed if antiferromagnetic long-range order is taken into account [61].

As noted previously [47], the interval $-0.2 \lesssim x \lesssim 0.25$, to which superconductivity is confined according to our variational study, corresponds to densities where the Fermi surface passes through the boundary of the folded Brillouin zone, at so-called hot spots. This means that parts of the Fermi surface are connected by wave vectors close to $\boldsymbol{Q} = (\pi, \pi)$, for which the magnetic structure factor has a pronounced peak [47], reminiscent of long-range antiferromagnetic order at half filling. This observation lends support to a magnetic pairing mechanism. In fact, an effective attraction of the form $-(U^2/t)\,\chi_0(\boldsymbol{k}+\boldsymbol{k}')$ is deduced using second-order perturbation theory for the effective particle–particle vertex [10], where $\chi_0(\boldsymbol{q})$ is the spin susceptibility for non-interacting electrons and the incoming and outgoing electrons have wave vectors $\pm\boldsymbol{k}$ and $\pm\boldsymbol{k}'$, respectively. A similar expression for the effective attraction, $-\frac{3}{2}(\bar{U}^2/t)\,\chi(\boldsymbol{q}, \omega)$, has been fitted to the particle–particle vertex calculated with the quantum cluster method [65], with a density- and temperature-dependent coupling constant $\bar{U}$ and the numerically calculated spin susceptibility $\chi(\boldsymbol{q}, \omega)$.

6. Summary and concluding remarks

In this paper, we have analysed various variational wave functions in the context of the 2D Hubbard model. Both antiferromagnetic ground states (at half filling) and superconducting ground states with d-wave symmetry (away from half filling) have been studied. We have considered states of the general form

$$|\Psi\rangle = \hat{P}|\Psi_0\rangle, \tag{40}$$

where $|\Psi_0\rangle$ is the ground state of an appropriate mean-field Hamiltonian, which includes a variational parameter Δ, the gap parameter. The operator $\hat{P}$ is unity in the simple mean-field theory, it consists of a single operator, $\hat{P} = \mathrm{e}^{-g\hat{D}}$, in the Gutzwiller ansatz or of several operators in more refined wave functions. The optimized gap parameter was found to depend sensitively on the choice of the wave function. It decreases by about an order of magnitude when proceeding from the simple mean-field theory to our favourite ansatz with $\hat{P} = \mathrm{e}^{-h\hat{H}_0/t}\mathrm{e}^{-g\hat{D}}$. Therefore Δ, taken as a variational parameter in wave functions of the form (40), cannot be identified with a physical energy gap (except in the simple BCS case where Δ is the minimum energy for adding an electron to the system), nor can it be associated with a characteristic energy scale such as $k_\mathrm{B}T^*$ (where T^* is the so-called pseudogap temperature [18, 21]). In contrast, the order parameter was found to depend little on the sophistication of the variational ansatz.

To our knowledge, there is no rigorous proof for the existence of long-range antiferromagnetic order in the 2D Hubbard model at half filling (nor in the case of the spin-$\frac{1}{2}$ Heisenberg model), although this question is not strongly debated. The case of (d-wave) superconductivity is much more controversial. Both the relatively small disparities between the order parameters obtained with different variational states close to half filling and the generally good agreement between our results and those of completely different approaches, quantum cluster [61] and Gaussian Monte Carlo [64], give rather strong support for the existence of d-wave superconductivity in the Hubbard model on a square lattice. Nevertheless, as we have seen in the simple example of the Hubbard square, our wave function is probably not optimal for the large value of U used in our calculations (and believed to be appropriate for the cuprates). Progress with complementary wave functions (linked to the $U \to \infty$ limit) or with other methods would be highly desirable.

Acknowledgments

We are grateful for financial support from the Swiss National Science Foundation through the National Centre of Competence in Research 'Materials with Novel Electronic Properties—MaNEP'.

References

[1] Kohn W and Luttinger J M 1965 *Phys. Rev. Lett.* **15** 524
[2] Anderson P W 1987 *Science* **235** 1196
[3] Mishchenko A S, Nagaosa N, Shen Z-X, De Filippis G, Cataudella V, Devereaux T P, Bernhard C, Kim K W and Zaanen J 2008 *Phys. Rev. Lett.* **100** 166401
[4] Giustino F, Cohen M L and Louie S G 2008 *Nature* **452** 975
[5] Reznik D, Sangiovanni G, Gunnarsson O and Devereaux T P 2008 *Nature* **455** E6

[6] Binz B, Baeriswyl D and Douçot B 2003 *Ann. Phys. Lpz.* **12** 704
[7] Zanchi D and Schulz H J 2000 *Phys. Rev.* B **61** 13609
[8] Halboth C J and Metzner W 2000 *Phys. Rev.* B **61** 7364
[9] Honerkamp C and Salmhofer M 2001 *Phys. Rev.* B **64** 184516
[10] Binz B, Baeriswyl D and Douçot B 2002 *Eur. Phys. J.* B **25** 69
[11] Anderson P W 1959 *J. Phys. Chem. Solids* **11** 26
[12] Chao K A, Spałek J and Oleś A M 1978 *Phys. Rev.* B **18** 3453
[13] Manousakis E 1991 *Rev. Mod. Phys.* **63** 1
[14] Lee P A, Nagaosa N and Wen X-G 2006 *Rev. Mod. Phys.* **78** 17
[15] Ogata M and Fukuyama H 2008 *Rep. Prog. Phys.* **71** 036501
[16] Gros C 1988 *Phys. Rev.* B **38** 931
[17] Yokoyama H and Shiba H 1988 *J. Phys. Soc. Japan* **57** 2482
[18] Paramekanti A, Randeria M and Trivedi N 2004 *Phys. Rev.* B **70** 054504
[19] Pathak S, Shenoy V B, Randeria M and Trivedi N 2009 *Phys. Rev. Lett.* **102** 027002
[20] Pauling L 1967 *The Nature of the Chemical Bond* (Ithaca, NY: Cornell University Press)
[21] Anderson P W, Lee P A, Randeria M, Rice T M, Trivedi N and Zhang F C 2004 *J. Phys.: Condens. Matter* **16** R755
[22] Coldea R, Hayden S M, Aeppli G, Perring T G, Frost C D, Mason T E, Cheong S-W and Fisk Z 2001 *Phys. Rev. Lett.* **86** 5377
[23] Katanin A A and Kampf A P 2002 *Phys. Rev.* B **66** 100403
[24] Müller-Hartmann E and Reischl A 2002 *Eur. Phys. J.* B **28** 173
[25] Katanin A A and Kampf A P 2003 *Phys. Rev.* B **67** 100404
[26] Comanac A, de' Medici L, Capone M and Millis A J 2008 *Nat. Phys.* **4** 287
[27] Aebi P, Osterwalder J, Schwaller P, Schlapbach L, Shimoda M, Mochiko T and Kadowaki K 1994 *Phys. Rev. Lett.* **72** 2757
[28] Borisenko S V, Golden M S, Legner S, Pichler T, Dürr C, Knupfer M, Fink J, Yang G, Abell S and Berger H 2000 *Phys. Rev. Lett.* **84** 4453
[29] Norman M R, Randeria M, Ding H and Campuzano J C 1995 *Phys. Rev.* B **52** 615
[30] Kim C, White P J, Shen Z-X, Tohyama T, Shibata Y, Maekawa S, Wells B O, Kim Y J, Birgenau R J and Kastner M A 1998 *Phys. Rev. Lett.* **80** 4245
[31] Dagotto E 1994 *Rev. Mod. Phys.* B **66** 763
[32] Troyer M and Wiese U-J 2005 *Phys. Rev. Lett.* **94** 170201
[33] Corney J F and Drummond P D 2006 *Phys. Rev.* B **73** 125112
[34] Corboz B, Troyer M, Kleine A, McCulloch I P, Schollwöck U and Assaad F F 2008 *Phys. Rev.* B **77** 085108
[35] Georges A, Kotliar G, Krauth W and Rozenberg M J 1996 *Rev. Mod. Phys.* **68** 13
[36] Maier T, Jarrell M, Pruschke T and Hettler M H 2005 *Rev. Mod. Phys.* **77** 1027
[37] Sénéchal D 2008 An introduction to quantum cluster methods arXiv:0806.2690
[38] Park H, Haule K and Kotliar G 2008 *Phys. Rev. Lett.* **101** 186403
[39] Gutzwiller M C 1963 *Phys. Rev. Lett.* **10** 159
[40] Coppersmith S N and Yu C C 1989 *Phys. Rev.* B **39** 11464
[41] Yokoyama H and Shiba H 1990 *J. Phys. Soc. Japan* **59** 3669
[42] Kaplan T A, Horsch P and Fulde P 1982 *Phys. Rev. Lett.* **49** 889
[43] Yokoyama H, Tanaka Y, Ogata M and Tsuchiura H 2004 *J. Phys. Soc. Japan* **73** 1119
[44] Tocchio L F, Becca F, Parola A and Sorella S 2008 *Phys. Rev.* B **78** 041101(R)
[45] Tahara D and Imada M 2008 *J. Phys. Soc. Japan* **77** 114701
[46] Eichenberger D and Baeriswyl D 2007 *Phys. Rev.* B **76** 180504(R)
[47] Eichenberger D and Baeriswyl D 2009 *Phys. Rev.* B **79** 100510(R)
[48] Otsuka H 1992 *J. Phys. Soc. Japan* **61** 1645
[49] Baeriswyl D 1987 *Springer Series in Solid-State Sciences* vol 69 (Berlin: Springer) p 183

[50] Sorella S, Martins G B, Becca F, Gazza C, Capriotti L, Parola A and Dagotto E 2002 *Phys. Rev. Lett.* **88** 117002
[51] Dzierzawa M, Baeriswyl D and Di Stasio M 1995 *Phys. Rev.* B **51** 1993
[52] Dzierzawa M, Baeriswyl D and Martelo L M 1997 *Helv. Phys. Acta* **70** 124
[53] Martelo L M, Dzierzawa M, Siffert L and Baeriswyl D 1997 *Z. Phys.* B **103** 335
[54] Baeriswyl D 2000 *Found. Phys.* **30** 2033
[55] Lieb E H 1989 *Phys. Rev. Lett.* **62** 1201
[56] Scalapino D J and Trugman S A 1996 *Phil. Mag.* B **74** 607
[57] Hirsch J E 1983 *Phys. Rev.* B **28** 4059
[58] Eichenberger D 2008 Superconductivity and antiferromagnetism in the two-dimensional Hubbard model *PhD Thesis* University of Fribourg, unpublished
[59] Hirsch J E and Tang S 1989 *Phys. Rev. Lett.* **62** 591
[60] Sandvik A W 1997 *Phys. Rev.* B **56** 11678
[61] Kancharla S S, Kyung B, Sénéchal D, Civelli M, Capone M, Kotliar G and Tremblay A-M S 2008 *Phys. Rev.* B **77** 184516
[62] Eichenberger D and Baeriswyl D 2007 *Physica* C **460** 1153
[63] Giamarchi T and Lhuillier C 1991 *Phys. Rev.* B **43** 12943
[64] Aimi T and Imada M 2007 *J. Phys. Soc. Japan* **76** 113708
[65] Maier T A, Macridin A, Jarrell M and Scalpino D J 2007 *Phys. Rev.* B **76** 144516